Evidence for excitonic polarons in InAs/GaAs quantum dots

V. Preisler, T. Grange, R. Ferreira, L. A. de Vaulchier, and Y. Guldner
Laboratoire Pierre Aigrain, Ecole Normale Supérieure, 24 rue Lhomond, 75231 Paris Cedex 05, France

F. J. Teran and M. Potemski
Grenoble High Magnetic Field Laboratory, CNRS/MPI, 25 avenue des Martyrs, 38042 Grenoble Cedex 9, France

A. Lemaître
Laboratoire de Photonique et Nanostructures, Route de Nozay, 91460 Marcoussis, France
(Received 9 December 2005; published 14 February 2006)

We investigate the interband transitions in several ensembles of self-assembled InAs/GaAs quantum dots by using photoluminescence excitation spectroscopy under strong magnetic fields up to 28 T. Well-defined resonances are observed in the spectra. The magnetic field dependence of the resonance energies allows an unambiguous assignment of the interband transitions which involve both discrete states of the quantum dots and wetting layer states. A strong anticrossing between two transitions is observed in all samples, which cannot be accounted for by a purely excitonic model. The coupling between the mixed exciton-longitudinal optical (LO) phonon states is calculated using the Fröhlich Hamiltonian. The excitonic polaron energies as well as the oscillator strengths of the interband transitions are determined. An anticrossing is predicted when two exciton-LO phonon states have close enough energies with phonon occupations which differ by one. A good agreement is found between the calculations and the experimental data evidencing the existence of excitonic polarons.

DOI: 10.1103/PhysRevB.73.075320 PACS number(s): 73.21.La, 71.38.−k, 78.67.Hc, 78.20.Ls

I. INTRODUCTION

Carrier-phonon interactions in semiconductor quantum dots (QDs) have attracted considerable attention because they are essential to understand the electronic properties of such a system, for instance, the carrier relaxation which is of particular interest in QDs. Various experimental and theoretical results have demonstrated that carriers confined in InAs/GaAs QDs are strongly coupled to the longitudinal optical (LO) vibrations of the underlying semiconductor lattice.[1–7] For electrons, this coupling leads to the formation of the so-called electron polarons which are the true excitations of a charged dot. The electron polarons have been extensively studied by far-infrared (FIR) magnetoabsorption in *n*-doped QDs as intraband optical transitions probe directly the polaron levels instead of the purely electronic states.[1,4] Similarly, hole polarons were recently evidenced in *p*-doped QDs by using FIR intraband magneto-optical experiments.[8] Optical interband transitions between valence and conduction QD states involve electron-hole pairs which are electrically neutral. Since the coupling between carriers and optical phonons is basically electrical (Fröhlich interaction), one could expect a rather small coupling between LO phonons and excitons. However, recent theoretical works have shown that excitons in QDs strongly couple to LO phonons in spite of their electrical neutrality.[9,10] The eigenstates of the interacting exciton and phonon systems are the so-called excitonic polarons which have important consequences on the understanding of the behavior of excited QDs. In particular, a reexamination of the energy relaxation paths of excited QDs and of the decoherence effects is needed.[5,11] Excitonic polarons are predicted to give significant modifications of the energy levels and large anticrossings when two exciton-phonon states have close enough energies with phonon occupations which differ by one. Such effects should be observed in the magnetic field dependence of the interband transitions, where the applied magnetic field is used to tune the energy separation between the various exciton-phonon states. However, interband transitions in a QD ensemble are inhomogeneously broadened because of size and composition fluctuations, so that no direct evidence for the formation of excitonic polarons has been reported so far. The experimental verification of the theoretical predictions thus requires overcoming the inhomogeneous broadening of the optical spectra, for instance, by using single QD spectroscopy.[12] In the present work, we have studied, at $T=4$ K, the photoluminescence excitation (PLE) under strong magnetic field up to 28 T of several ensembles of self-assembled InAs/GaAs QDs. Undoped, *n*-doped, and *p*-doped high quality samples have been investigated. PLE spectroscopy probes the absorption of a subensemble of similar QDs defined by the detection energy and thus allows one to circumvent part of the inhomogeneous broadening. Several well-defined resonances are observed in all samples. The magnetic field dependence of the resonance energies allows an unambiguous assignment of the interband transitions. PLE spectra display transitions between the discrete states of the QDs as well as transitions involving the wetting layer states. A strong anticrossing between two transitions is observed in all samples as the magnetic field is changed. Such an anticrossing cannot be accounted for by a purely excitonic model and one has to consider the exciton-lattice interactions. We have calculated the coupling between the mixed exciton-LO phonon states using the Fröhlich Hamiltonian and we have determined the excitonic polaron states as well as the energies and oscillator strengths of the interband transitions. A good

agreement is found between these calculations and the experimental data, evidencing the existence of excitonic polarons.

II. EXPERIMENTAL DETAILS

The series of QD samples investigated here, labeled An (n=1,2,3), was grown on (001) GaAs substrates by molecular beam epitaxy using the Stranski-Krastanov mode of InAs on GaAs.[13] Each sample contains a multistack of 20 layers of InAs QDs separated by 50 nm barriers, each layer having a QD density of $\sim 4\times 10^{10}$ cm^{-2}. The InAs QDs were formed by depositing 2.2 monolayers (ML) at 520 °C with a growth rate of 0.12 ML/s. There were no growth interruptions before GaAs overgrowth. The doping was varied from sample to sample, all the other growth parameters being exactly the same. Sample A1 was undoped while samples A2 and A3 present a δ-doping of the GaAs barriers at 2 nm under the dot layers. Sample A2 was n-doped with a Si δ-doping concentration of $\sim 4\times 10^{10}$ cm^{-2} while A3 was p-doped with a Be δ-doping concentration of $\sim 4\times 10^{10}$ cm^{-2}. The samples were characterized by photoluminescence (PL) and by FIR magnetospectroscopy at 2 K. The PL peak, in all samples, was centered at 1.2 eV with a full width at half maximum (FWHM) of ~50 meV. An energy separation of ~47 meV (~22 meV) between the ground and the first excited conduction (valence) states was measured by FIR magnetospectroscopy in samples similar to A2 (A3). Cross-sectional transmission electron spectroscopy in samples grown in similar conditions have shown that the QDs resemble flat truncated cones with a ~20 nm basis diameter and a ~3 nm height.[14] We have performed low temperature (T=4 K) interband measurements on these QD ensembles using PL and PLE techniques under strong magnetic field applied along the sample growth axis. Measurements up to 28 T have been done at the High Magnetic Field Laboratory in Grenoble. The samples were mounted in a resistive magnet and immersed in liquid helium. For the PLE measurements, a Ti:sapphire laser was used. A system of optical fibers was used for the sample excitation and the collection of the PLE signal. The emitted light from the sample is dispersed through a Jobin Yvon spectrometer and detected by a charge coupled device camera.

III. RESULTS

Interband transitions of a QD ensemble are inhomogeneously broadened because of fluctuations of the confining potential which arise from size and composition dispersion. The broad bell-like form of a PL peak is more or less a measure of size inhomogeneity. PLE measurements permit the selection of a subensemble of similar sized dots from a sample containing a range of dot sizes.[15] The subensemble investigated in a PLE measurement is defined by fixing a narrow detection energy window, E_{det}, within the broadened PL peak, while the excitation optical energy, E_{exc}, is varied. As the PL peak at 4 K of our samples is centered at ~1200 meV, we have chosen detection energies in the range 1190–1217 meV. Although such spectra are still inhomogeneously broadened due to shape and composition variation, well-defined features are usually observed, making low-temperature PLE spectroscopy an appropriate probe of the energy states of QDs. Figure 1 depicts the PLE spectra of sample A3 for detection energies E_{det}=1194, 1206, and 1215 meV at 4 K. The x-axis shows the excess excitation energy $\Delta E=E_{exc}-E_{det}$. The same four features, indicated by arrows in Fig. 1, are observed for all three detection energies. A low-energy peak is observed at ~50 meV, a second peak is found at ~75 meV, a third peak is found at ~110 meV, and finally a strong peak is observed at ~220 meV.

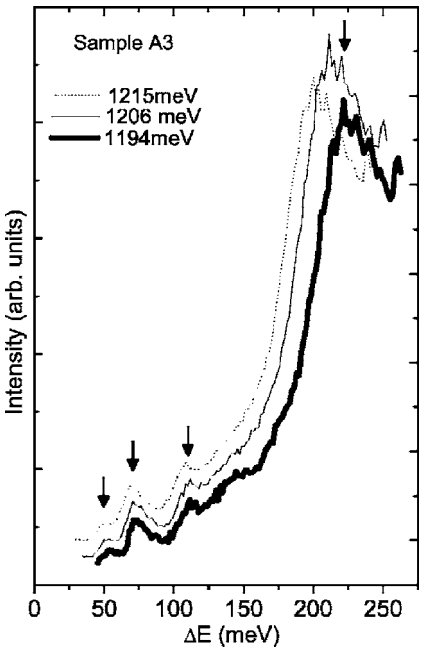

FIG. 1. Normalized PLE spectra of the A3 sample taken at 4 K for E_{det}=1194, 1206, and 1215 meV, where $\Delta E=E_{exc}-E_{det}$.

We attribute this last high-energy peak to the excitation resonance of the wetting layer (WL). The energy, ΔE, of this peak decreases as the detection energy is increased, however, the transition energy, $\Delta E+E_{det}$, stays at the nearly constant energy of 1420 meV. Such an energy is typical given the growth conditions used for our samples and corresponds to a few monolayer thick InAs WL. As the thickness of the WL stays more or less constant throughout the sample, the WL excitation energy should also remain constant.

The remaining three peaks, found at lower energies, are associated with transitions between bound levels in the QDs. For QDs with a perfect cylindrical symmetry, the ground and first excited state in both the conduction and valence band are s- and p-like, respectively. In order to associate the excitation peaks with transitions in the QDs, a magnetic field B is applied along the sample's growth axis, as it is well-known that the effect of a magnetic field is different for s, p, and d states. Figure 2 displays the magneto-PLE spectra of sample A3 recorded at 4 K from B=0 to 28 T every 4 T and for a detection energy of 1215 meV. Similar results were observed for all samples as shown in Fig. 3 where the magneto-PLE spectra for samples A1, A2, and A3 are depicted on a magnified scale. The energy of the PLE peaks as a function of magnetic field is plotted in Fig. 4 for sample A3. As the

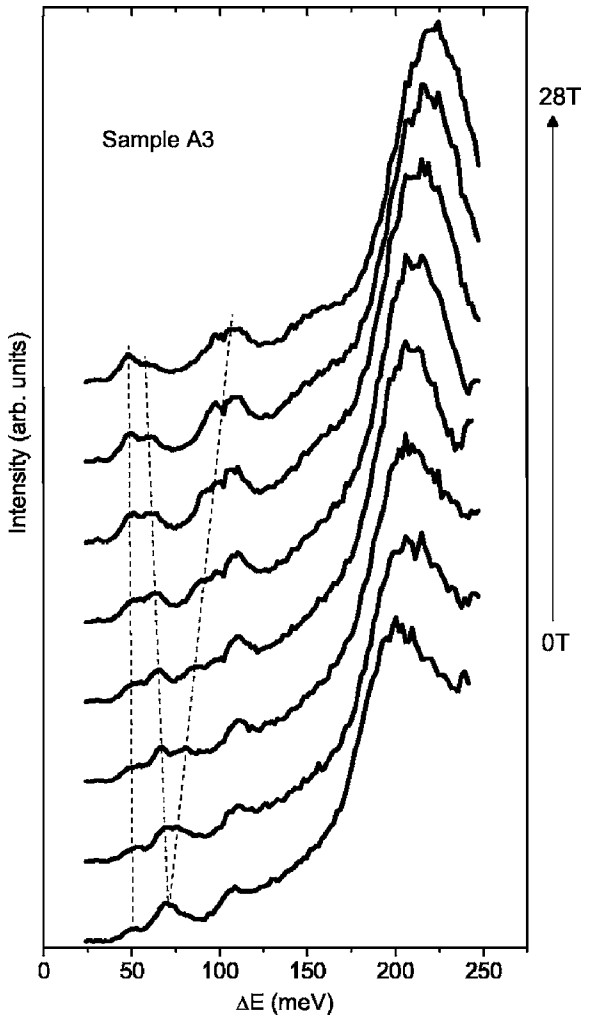

FIG. 2. Magneto-PLE spectra of the A3 sample recorded at 4 K from $B=0$ to 28 T every 4 T and for a $E_{dect}=1215$ meV. Traces have been vertically offset for clarity. The dashed lines are guides for the eyes.

magnetic field increases, the peak that was initially at 75 meV splits into two separate peaks: one peak that increases in energy and a second peak that decreases in energy. These peaks can be associated with p-like transitions. This association is made because firstly the peaks move with the magnetic field, which is characteristic of p-states, and secondly the energy at 0 T of these peaks roughly corresponds to the addition of the experimentally obtained s-p energy transitions of holes and electrons. The remaining two peaks at 50 and 110 meV stay nearly constant with the increasing magnetic field. We therefore associate these peaks with transitions involving states whose energies move very little with an applied magnetic field, for instance, s-states or eventually p_h-states. Finally, the peak at 220 meV increases in energy with the increasing magnetic field. This is the expected behavior for a WL transition in a magnetic field. Indeed, using a WL electron mass $m_e=0.07m_o$ and a heavy hole mass $m_h=0.22m_o$, a slope of

$$\frac{1}{2}\hbar e(m_e^{-1}+m_h^{-1})=1.1 \text{ meV T}^{-1} \quad (1)$$

is expected for the WL absorption, which approximately corresponds to the PLE spectra where we measure a slope of 0.8 meV T^{-1}. This reinforces our earlier assumption that this peak is associated with a WL conduction band-WL valence band transition.

Let us now take a closer look at the oscillator strengths of the lower energy peaks, as shown in Fig. 3. At 0 T, the intensity of the low-energy peak at 50 meV is about 20% of that of the 75 meV peak. As the magnetic field increases, an exchange of oscillator strength between these two peaks is observed. For samples A1 and A3, at 20 T the two peaks have the same intensity and by 24 T the oscillator strength of the low-energy peak has surpassed that of its neighbor. For sample A2, the energy difference between the two peaks at 0 T is smaller and therefore the anticrossing is observed at a lower magnetic field. Such a behavior can not be explained using a purely electronic model. It is necessary to use a model that takes into account the coupling between the optical phonons and the photo-created electron-hole pair in the QD. Such a model is presented in the next section.

IV. ANALYSIS AND DISCUSSION

In order to predict the optical properties of an exciton in interaction with LO phonons, we use the following Hamiltonian:

$$H=H_e(B)+H_h(B)+V_{e\text{-}h}+H_{ph}+V_F, \quad (2)$$

where H_e and H_h are the electron and hole Hamiltonians with an applied magnetic field B, $V_{e\text{-}h}$ is the electron-hole Coulomb interaction, H_{ph} is the LO phonon Hamiltonian, and V_F is the Fröhlich Hamiltonian. Before dealing with the electron phonon interaction, we first describe the electronic part of the Hamiltonian, i.e., the first two terms in Eq. (2).

We model the QDs by a truncated $Ga_xIn_{1-x}As$ cone of height h and with a circular basis of radius R resting on a thin layer of the same material and inserted in a GaAs matrix. The electron and hole levels are calculated within a one-band model.[1,8] Due to the cylindrical symmetry along the growth (z) direction, the electronic and hole levels are labeled by the projection of their angular momentum l_z along this axis: s states ($l_z=0$), p states ($l_z=0\pm1$),…. For the investigation of the low-energy interband transitions, we may limit our description to the first low-lying conduction and valence bound levels ($l_z=0,\pm1$).

The effect of a magnetic field is to introduce both a Zeeman shift proportional to l_z and a d iamagnetic shift proportional to the squared extent of the confined in-plane orbit. The Zeeman shift allows a clear discrimination between the dot states. This controlled selective tuning of the different interband transitions is of crucial importance in our study, since a clear assignment of the different interband lines is often difficult in experiments with a dot ensemble at zero field.

Self-assembled QDs are known to display a slight in-plane anisotropy. Different effects have been considered in

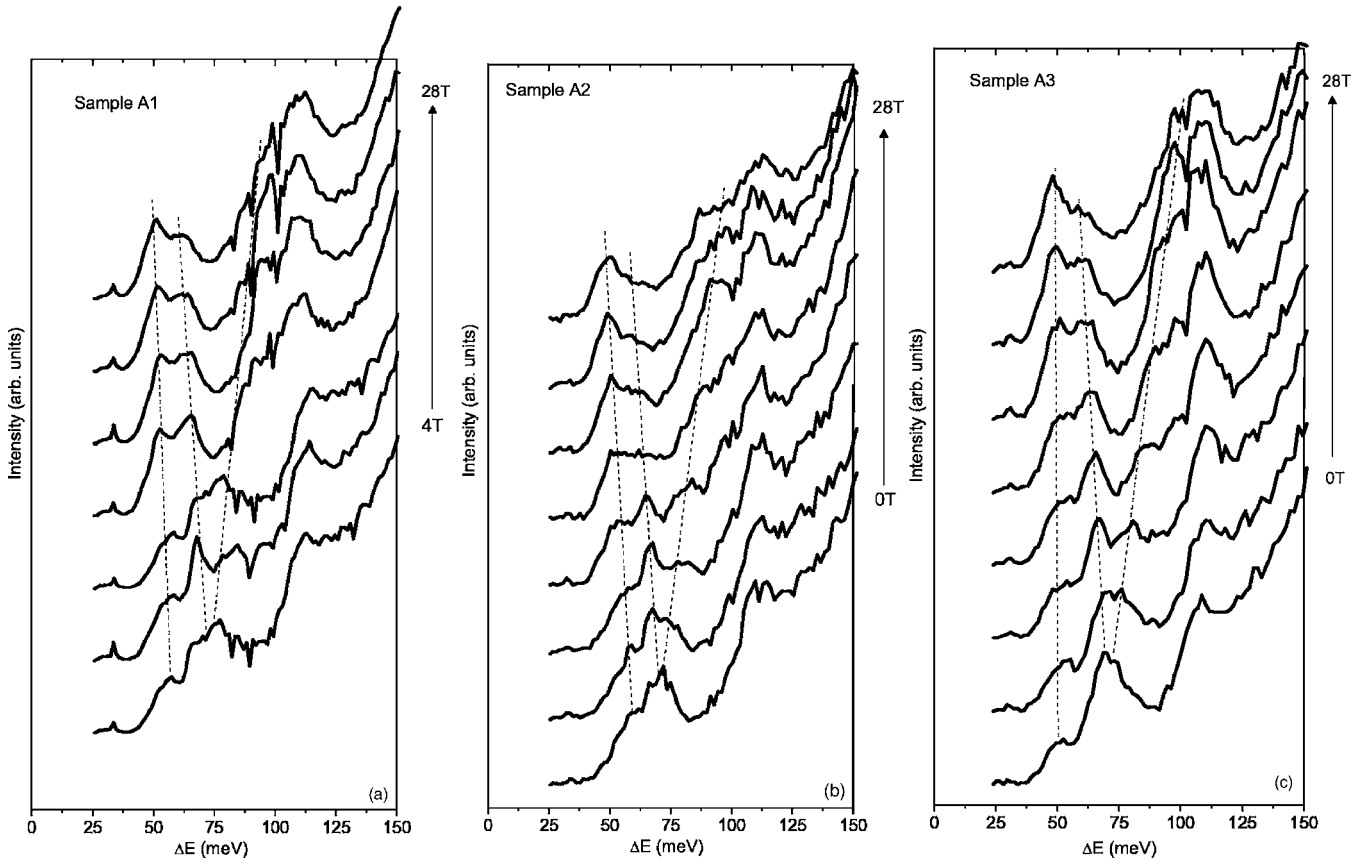

FIG. 3. Magneto-PLE spectra of samples A1 (a), A2 (b), and A3 (c) at 4 K from $B=0$ to 28 T every 4 T and for a $E_{dect}=1215$ meV. The dashed lines are guides for the eyes.

the literature, running from intrinsic couplings that are better handled within first-principle and/or many-band calculations involving a detailed description of the underlying materials forming the QD,[16] to the more phenomenological shape anisotropy[17] contribution for the carriers confinement potential that has been considered in the framework of the one-band envelope function formalism.[1] In any case, the main effect of the anisotropy is to split the two degenerate $l_z=\pm 1$ levels of the QD. The splitting of the two levels at $B=0$ T is clearly observed in the FIR absorption of doped QDs: ~ 5 meV for electrons and ~ 2 meV for holes.[1,8] In our cylindrical basis, the in-plane anisotropy is treated in perturbation by introducing couplings between p^+ and p^- states equal to half of the splitting observed in intraband spectroscopy.

The strong coupling of both electrons and holes to optical phonons has been evidenced in previous works. The main point is that electronic and lattice excitations strongly mix to form polaron states in quantum dots. From the theoretical point of view, the QD polaron states reflect a complex entanglement of exciton and phonon states. This complex coupling is described by the Fröhlich Hamiltonian, which for an exciton reads

$$V_F = \sum_{\mathbf{r}_e,\mathbf{r}_h} \sum_{\mathbf{q}} \frac{A_F}{q} (e^{i\mathbf{q}\cdot\mathbf{r}_e} - e^{i\mathbf{q}\cdot\mathbf{r}_h})(a_{\mathbf{q}} - a^+_{-\mathbf{q}}), \tag{3}$$

where $a_{\mathbf{q}}$ and $a^+_{\mathbf{q}}$ are the annihilation and creation operator for a LO phonon with momentum $\mathbf{q}$, and $\mathbf{r}_e$ and $\mathbf{r}_h$ are the position operators for electrons and holes. The term A_F includes in its definition the Fröhlich constant which is taken as $\alpha=0.11$, consistent with precedent polaron studies in QDs.[1]

The noninteracting exciton-phonon states in an uncoupled system are labeled $|n_e,n_h,N_{\mathbf{q}}\rangle$, where $|n\rangle=|s\rangle,|p^{\pm}\rangle$ are purely electronic levels. $|N_{\mathbf{q}}\rangle$ denotes the ensemble of the N LO-phonon states in the $\{\mathbf{q}\}$ modes. The Fröhlich Hamiltonian couples states which differ by one phonon.

$$\langle n_e,n_h,0|V_F|n'_e,n'_h,1_{\mathbf{q}}\rangle = \frac{A_F}{q}[\delta_{n_h n'_h} v_{n_e n'_e}(\mathbf{q}) - \delta_{n_e n'_e} v_{n_h n'_h}(\mathbf{q})], \tag{4}$$

where $v_{nn'}(\mathbf{q})=\langle n|e^{i\mathbf{q}\cdot\mathbf{r}}|n'\rangle$. Nonvanishing coupling occurs only between states with either the same electron or the same hole wave functions.

Here we present the calculation of excitonic polarons in the energy range (40–100 meV) relevant to interpret the anticrossing observed in the PLE spectra. We have used the dispersionless LO phonon approximation, which allows the very accurate calculation of polaron levels in QDs.[1] An LO phonon energy of $\hbar\omega=36$ meV has been used. We have taken into account all nonvanishing Fröhlich coupling terms as well as anisotropy and Coulomb interactions (with a dielectric constant $\epsilon=12.5$). The energy dispersions and oscillator strengths of the polaron states, presented in Fig. 5, were calculated using an in-plane effective mass for electrons m_e

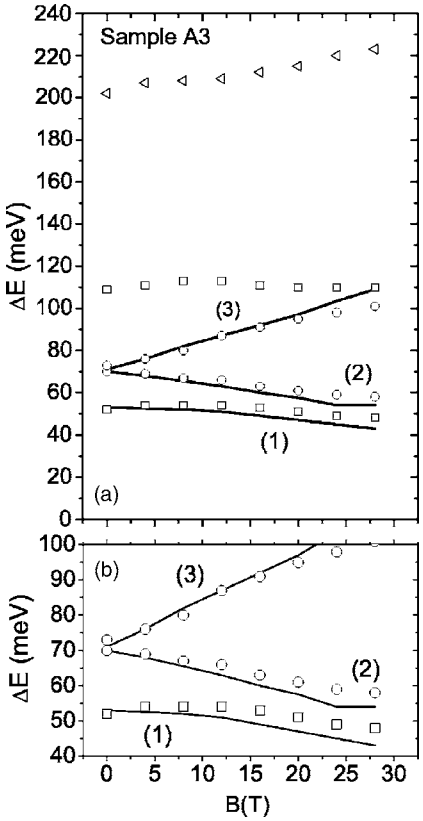

FIG. 4. Magnetic field dispersion of PLE resonances in sample A3 in open figures with the calculated energy transitions in solid lines (a) and a zoom (b) of the polaron states (1), (2), and (3), as labeled in Fig. 5. See Sec. IV for details and parameters of the calculated fit.

$=0.07m_o$ and for holes $m_h=0.22m_o$. These values were fixed in order to agree with FIR intraband magnetospectrocopy results. The other dots parameters were chosen in order to fit the experimental values of both the intraband *s-p* electronic (hole) transitions [47 meV(22 meV)] and the interband ground state energy (detection energy of 1215 meV). The parameters resulting from the fit are the following: cone with a radius $R=115$ Å and height $h=28$ Å, and conduction (valence) band offset of 290 meV (212 meV). The dot size is consistent with direct size measurement[14] and the band offsets are compatible with an average gallium content of $x \simeq 0.5$ in the QDs.

In Fig. 5(b) the solid lines represent the calculated energy transitions for an uncoupled system, where the zero energy has been taken at the ground state ($|s_e,s_h,0\rangle$). We represent in this figure only the two principal exciton-phonon states, $|p_e^-,p_h^+,0\rangle$ and $|s_e,p_h^+,1_{\mathbf{q}}\rangle$, which are responsible for the experimentally observed anticrossing. The $|p_e^-,p_h^+,0\rangle$ state displays a strong negative Zeeman slope with the magnetic field and crosses the one phonon continuum $|s_e,p_h^+,1_{\mathbf{q}}\rangle$ for a magnetic field of around 20 T. Within the approximation of dispersionless phonons, the Fröhlich coupling between the purely electronic state $|p_e^-,p_h^+,0\rangle$ and the one phonon continuum $|s_e,p_h^+,1_{\mathbf{q}}\rangle$ can be treated in a two discrete level scheme: one discrete mode of the phonon continuum (labeled 1_{α_1}) is coupled with strength V_{int} to the discrete purely

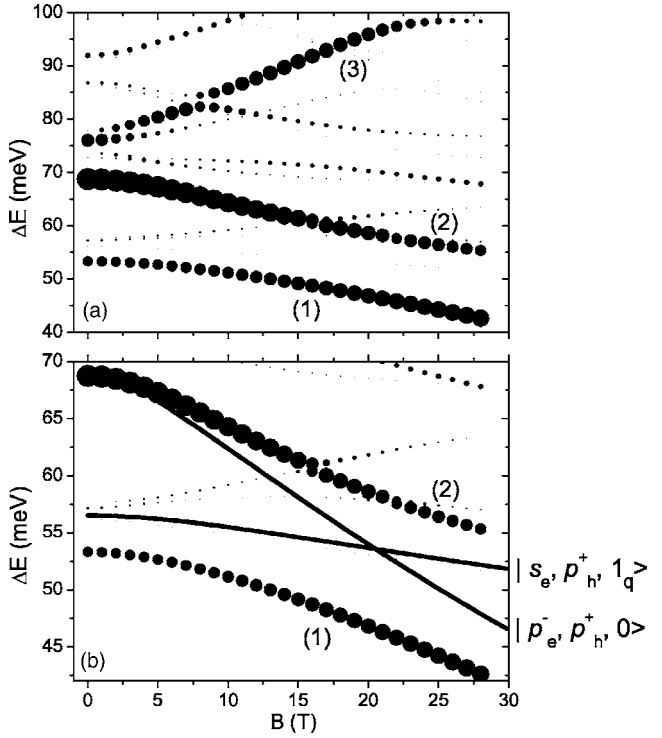

FIG. 5. Calculated excitonic polaron energies and intensities as a function of the magnetic field (a) and a zoom (b) of the anticrossing between polaron states (1) and (2). The solid lines in (b) correspond to noninteracting exciton-phonon states. The area of the circles is proportional to the oscillator strengths.

electronic state while the remaining orthogonal space is left uncoupled (see the Appendix of Ref. 8). In the two-level basis ($|p_e^-,p_h^+,0\rangle,|s_e,p_h^+,1_{\alpha_1}\rangle$), the Hamiltonian reads

$$H=\begin{pmatrix} E_{p_e^-p_h^+}(B) & V_{int} \\ V_{int} & E_{s_ep_h^+}(B)+\hbar\omega_{LO} \end{pmatrix}. \tag{5}$$

The coupling term V_{int} was calculated and found to be 6 meV. The eigenstates of this Hamiltonian are the polarons labeled (1) and (2) in Figs. 5(a) and 5(b). A large anticrossing of $2V_{int}$ is seen between these two polaron states. The surface area of the circles in the figure are proportional to the oscillator strength of a given polaron transition at a certain magnetic field. The calculation of these oscillator strengths is described below.

In Fig. 5(a) we present all the calculated polaron energy transitions in a larger energy range. Since the different Fröhlich coupling terms involve different phonon modes we introduce five additional modes labeled 1_{α_i} ($i=2,\ldots,6$). This gives us a Hamiltonian in a basis containing 21 discrete states: 4 purely excitonic states $|p_e^{\pm},p_h^{\pm},0\rangle$, 16 excitonic states with one-phonon mode ($|s_e,p_h^{\pm},1_{\alpha_{i=1,2}}\rangle,|p_e^{\pm},s_h,1_{\alpha_{i=3,4}}\rangle$ and $|p_e^{\pm},p_h^{\pm},1_{\alpha_{i=5,6}}\rangle$), and the fundamental excitonic state with two-phonon modes $|s_e,s_h,2_{\alpha_1,\alpha_2}\rangle$. The numerical diagonalization of this Hamiltonian gives us the polaron energy transitions. The energy positions as a function of magnetic field are in good agreement with our data, as seen in Fig. 4.

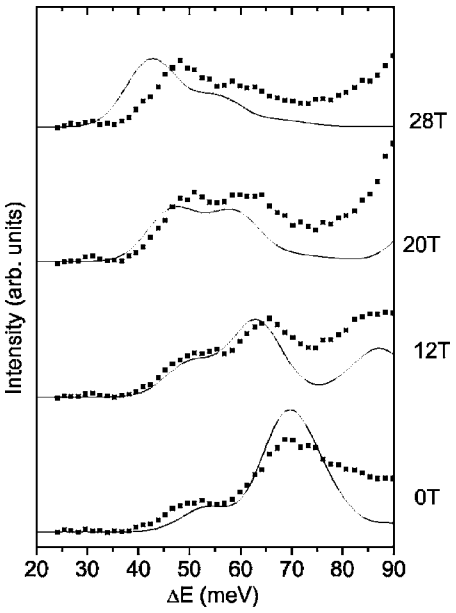

FIG. 6. Experimental (full squares) and calculated (solid lines) spectra for different magnetic fields. The experimental data was taken for an $E_{dect}=1215$ meV and for sample A3. The parameters used in the calculation are given in the text.

In the relevant energy range, the only optically active levels are $|p_e^-,p_h^+,0\rangle$ and $|p_e^+,p_h^-,0\rangle$. The oscillator strength of the given polaron state $|\psi\rangle$ is therefore proportional to its weight on these two states and reads

$$OS_{|\psi\rangle} \propto |\langle p_e^-,p_h^+,0|\psi\rangle + \langle p_e^+,p_h^-,0|\psi\rangle|^2 \tag{6}$$

since the two optically active states have the same oscillator strength. For the anticrossing represented in Fig. 5(b), the oscillator strengths of polarons (1) and (2) are roughly proportional to their weight on the $|p_e^-,p_h^+\rangle$ state. Hence we observe an exchange of oscillator strength between the two polarons as the magnetic field is increased.

Using Eq. (6), we calculate the interband absorptions. The solid lines in Fig. 6 represent the calculated absorption spectra at different magnetic fields. Each discrete level is replaced by a Gaussian peak with a FWHM of 12 meV in order to account for inhomogeneous broadening (i.e., fluctuations of dot dimensions in the subensemble of QDs defined by the detection energy). We compare our calculated interband absorption spectra with the PLE experimental data. The full squares are data points taken for sample A3 for an $E_{dect}=1215$ meV. The evolution of the oscillator strengths of the absorptions with the magnetic field is very well described by our model. We are able to predict the exchange of oscillator strength observed in our results demonstrating the validity of our analysis and the existence of excitonic polarons. Similar agreement is found for results obtained for samples A1 and A2. We point out that, in general, a PLE signal is not necessarily equivalent to an absorption spectrum. The very good agreement obtained here between the two is due to the short polaron relaxation time compared to interband radiative decay time. Far-infrared pump-probe spectroscopy experiments have demonstrated that intraband polaron decay time in InAs/GaAs QDs varies between 20 and 70 ps depending on the polaron energy.[18,19] Excitonic polaron relaxation times are expected to be on the same order of magnitude, the relaxation mechanism (due to phonon anharmonicity) being similar. Since interband radiative decay time is on the order of 1 ns, the relaxation process will always go through the ground exciton state. Hence the PLE is proportional to the absorption.

Finally, it is important to point out that our calculations, that consider neutrally charged dots, were also used to describe experimental results obtained from charged dots. When dealing with negatively (positively) charged QDs, one has to consider trions, i.e., two electrons (holes) and one hole (electron). If we study the low-energy excitation spectrum of charged QDs neglecting spin-dependent effects, the additional charge remains a spectator and the excitation spectrum resembles that of neutral QDs.[20] This could explain why samples A2 and A3 display PLE spectra which are quite similar to those recorded in sample A1.

V. CONCLUSION

In summary, we have investigated the interband transitions in several ensembles of self-assembled InAs/GaAs QDs by using PLE spectroscopy under a strong magnetic field. The magnetic field dependence of the interband transitions allows their unambiguous assignment, as the effect of a magnetic field is significantly different for s or p states. When two exciton-LO phonon states have close enough energies with phonon occupations which differ by one, a large anticrossing is theoretically predicted. Such a situation is experimentally induced in our samples by the applied magnetic field for the two interband transitions ($|p_e^-,p_h^+,0\rangle, |s_e,p_h^+,1_{\alpha_1}\rangle$) and a strong anticrossing is actually observed in all the investigated samples. We have calculated the coupling between the mixed exciton-LO phonon states using the Fröhlich Hamiltonian and we have determined the energies and oscillator strengths of the interband transitions. Our model accounts well for the experimental data, evidencing that the excitons and LO-phonons are in a strong coupling regime in QDs and the interband transitions occur between excitonic polaron states. Finally, we believe that the existence of excitonic polarons could present important consequences for the energy relaxation in excited QDs and for the coherence decay times of the fundamental optical transitions.

ACKNOWLEDGMENTS

The Laboratoire Pierre Aigrain is a "Unité Mixte de Recherche" (UMR 8551) between Ecole Normale Superieure, the University Pierre et Marie Curie (Paris 6), and the CNRS. This work was partially supported by the European Access Program (RITA-CT-2003-505474). We would like to thank G. Bastard and S. Hameau for very valuable and fruitful discussions.

[1] S. Hameau, J. N. Isaia, Y. Guldner, E. Deleporte, O. Verzelen, R. Ferreira, G. Bastard, J. Zeman, and J. M. Gérard, Phys. Rev. B **65**, 085316 (2002).
[2] D. Sarkar, H. P. van der Meulen, J. M. Calleja, J. M. Becker, R. J. Haug, and K. Pierz, Phys. Rev. B **71**, 081302(R) (2005).
[3] P. A. Knipp, T. L. Reinecke, A. Lorke, M. Fricke, and P. M. Petroff, Phys. Rev. B **56**, 1516 (1997).
[4] S. Hameau, Y. Guldner, O. Verzelen, R. Ferreira, G. Bastard, J. Zeman, A. Lemaître, and J. M. Gérard, Phys. Rev. Lett. **83**, 4152 (1999).
[5] O. Verzelen, R. Ferreira, and G. Bastard, Phys. Rev. B **62**, R4809 (2000).
[6] T. Inoshita and H. Sakaki, Phys. Rev. B **56**, R4355 (1997).
[7] X. Q. Li and Y. Arakawa, Phys. Rev. B **57**, 12285 (1998).
[8] V. Preisler, R. Ferreira, S. Hameau, L. A. de Vaulchier, Y. Guldner, M. L. Sadowski, and A. Lemaître, Phys. Rev. B **72**, 115309 (2005).
[9] O. Verzelen, R. Ferreira, and G. Bastard, Phys. Rev. Lett. **88**, 146803 (2002).
[10] R. Heitz, I. Mukhametzhanov, O. Stier, A. Madhukar, and D. Bimberg, Phys. Rev. Lett. **83**, 4654 (1999).
[11] X.-Q. Li, H. Nakayama, and Y. Arakawa, Phys. Rev. B **59**, 5069 (1999).
[12] R. Oulton, J. J. Finley, A. I. Tartakovskii, D. J. Mowbray, M. S. Skolnick, M. Hopkinson, A. Vasanelli, R. Ferreira, and G. Bastard, Phys. Rev. B **68**, 235301 (2003).
[13] L. Goldstein, F. Glas, J. Y. Marzin, M. N. Charasse, and G. Leroux, Appl. Phys. Lett. **47**, 1099 (1985).
[14] B. Grandidier, Y. M. Niquet, B. Legrand, J. P. Nys, C. Priester, D. Stiévenard, J. M. Gérard, and V. Thierry-Mieg, Phys. Rev. Lett. **85**, 1068 (2000).
[15] R. Heitz, O. Stier, I. Mukhametzhanov, A. Madhukar, and D. Bimberg, Phys. Rev. B **62**, 11017 (2000).
[16] G. Bester, S. Nair, and A. Zunger, Phys. Rev. B **67**, 161306(R) (2003).
[17] M. Fricke, A. Lorke, J. P. Kotthaus, G. Medeiros-Ribeiro, and P. M. Petroff, Europhys. Lett. **36**, 197 (1996).
[18] S. Sauvage, P. Boucaud, R. P. S. M. Lobo, F. Bras, G. Fishman, R. Prazeres, F. Glotin, J. M. Ortega, and J. M. Gérard, Phys. Rev. Lett. **88**, 177402 (2002).
[19] E. A. Zibik, L. R. Wilson, R. P. Green, G. Bastard, R. Ferreira, P. J. Phillips, D. A. Carder, J.-P. R. Wells, J. W. Cockburn, M. S. Skolnick, M. J. Steer, and M. Hopkinson, Phys. Rev. B **70**, 161305(R) (2004).
[20] M. E. Ware, E. A. Stinaff, D. Gammon, M. F. Doty, A. S. Bracker, D. Gershoni, V. L. Korenev, S. C. Badescu, Y. Lyanda-Geller, and T. L. Reinecke, Phys. Rev. Lett. **95**, 177403 (2005).